

*SOME RELATIONSHIPS GOVERNING THE P-T PHASE DIAGRAMS  
AND POLYMORPHIC TRANSFORMATIONS OF ELEMENTS UNDER HIGH PRESSURES*

V. V. EVDOKIMOVA

Institute for High-Pressure Physics, Academy of Sciences, U.S.S.R.

Usp. Fiz. Nauk **88**, 93-123 (January, 1966)

## 1. INTRODUCTION

CERTAIN properties of substances, such as their compressibility, melting point, thermal expansion coefficient, etc., exhibit, under normal conditions, a periodic dependence on the atomic number of the element.

Vereshchagin and Likhter<sup>[1]</sup> and, later, Ryabinin<sup>[2]</sup> showed that the general nature of the periodicity was retained up to pressures of 500 kbar, but with further increase in the pressure the periodic curve gradually smoothed out so that at very high pressures it became a monotonic function of the atomic number.<sup>[3]</sup> In other words, at very high pressures, elements cease to differ from one another in their chemical and physical properties.

It is known that two-thirds of the elements in the periodic system have atoms with unfilled inner shells and, as found experimentally, pressure is capable of transferring electrons to vacant levels of higher energies. Since different energies are needed to achieve these electronic transitions in different elements, they naturally occur at different pressures. The lowest pressure for an electronic transition known at present is that of cerium; an electronic transition from the 4f-state into the 5d-state takes place at only 7 kbar. A discontinuous change in the structure of the energy spectrum of electrons is accompanied by a discontinuous change in the electrical conductivity so that discontinuities in the electrical resistance under pressure may indicate electronic transitions. However, it must be stated that a discontinuous change in the electrical conductivity also accompanies a polymorphic transition in a substance, which is a change in the crystal lattice. X-ray-diffraction analysis, by means of which we can estimate the atomic volume before and after a transition, helps us to identify an electronic transition. For example, in the case of cerium, x-ray analysis shows that under a pressure of 7 kbar a discontinuous change in volume by 7.7% is not accompanied by a change in the crystal lattice: it remains fcc. However, an estimate of the ionic radii shows that for the same transition the ionic radius jumps from 1.85 to 1.71 Å.<sup>[4]</sup>

It is quite likely that the 42.5 kbar transition in cesium is also electronic. Cesium occupies a special place among other elements in that the 6s-, 5d-, and 4f-states of its electrons are extremely close in their energy values. It has been calculated that a pressure of 45-50 kbar should be sufficient to transfer the only

outer electron of cesium from the 6s- to the 4f-state and thus to convert cesium from a metal into an insulator. With further increase in the pressure, this electron may go over to the 5d-state and then cesium should again become a metal.<sup>[5]</sup> It is evident from Fig. 2 that a sudden rise in the electrical resistance is indeed observed at 42.5 kbar and that it is replaced by a sharp drop when the pressure is increased slightly.

In principle, electronic transitions are possible in all elements having unfilled levels. Theoretical calculations give estimates of 10-100 kbar for electronic transitions. It is obvious that the change in the structure of an atom induced by an electronic transition will lead to a complete change in the chemical properties since these are governed by the electronic structure of the outer shells. Under high-pressure conditions, we would expect a somewhat different periodic table of elements since the change in their properties will affect the positions of the elements in the periodic table.<sup>[6]</sup>

A further increase in the pressure will lead to the destruction of the electronic shells and the substance will go over to a plasma state with fixed positions of ("bare") nuclei or nuclei having electronic shell residues. Various theoretical estimates give different values for the pressures at which atoms and a crystal lattice would be destroyed. Relatively recent calculations made by Abrikosov<sup>[7]</sup> showed that the crystal lattice should be conserved at pressures up to 100,000 kbar, and that, when very highly compressed, all elements should have the same crystal lattice with the highest binding energy. At present, it is difficult to predict the type of lattice which strongly compressed elements should assume: it may be bcc, or fcc, or hcp, with the ratio of axes in the latter satisfying the condition of maximum binding energy.

Thus, working even with maximum practically realizable pressures, we are still dealing with crystalline substances having a crystal lattice. The unique form of the lattice which a strongly compressed substance should assume can be deduced by observing the sequence of transitions from one crystal lattice to another in each of the elements in the periodic table, subjected to rising pressure.

A change in the external conditions (pressure or temperature) may, in certain cases, alter the equilibrium stable state of a substance, which corresponds to a minimum of the thermodynamic potential. Further

changes in the pressure and temperature will make a substance assume a state of new stable equilibrium, i.e., it will cause a transition to a different phase. This process takes place when a substance is melted or its crystal structure changed. The boundary between two thermodynamically stable phases is the equilibrium curve on which these phases have equal thermodynamic potentials. Thus, by plotting on a plane the equilibrium curves between various phases of a substance in the coordinates of pressure  $P$  and temperature  $T$ , we obtain the  $P$ - $T$  phase diagram of this substance.

We cannot find the sequence followed by elements when one crystal structure is transformed into another under pressure without the use of the  $P$ - $T$  diagrams. The  $P$ - $T$  phase diagrams are now known for many elements. In considering the  $P$ - $T$  diagrams one after another in the sequence of elements in Mendeleev's periodic system, we observe a number of interesting features.\*

The first worth noting is the fact that the  $P$ - $T$  phase diagrams of elements of the same group are very similar and as the atomic number increases they gradually change. This change represents a shift of the diagrams toward lower pressures and lower temperatures; in some cases, for example, group IV-B elements, the diagrams are shifted to negative pressures. This feature, which is common to all groups in the periodic table, justifies one's predicting the possible form of the  $P$ - $T$  diagram of any element from a knowledge of the diagrams of its neighbors in the same group.

In considering the  $P$ - $T$  diagrams, we also note that the differences between elements are reflected in the variety of forms of the phase boundaries between various modifications. A consideration of the reasons for this variety—particularly the reasons for the negative slopes of the fusion curves and of the boundaries between solid phases—could be the subject of a special investigation but here we shall only consider one facet of this subject.

The nature of the pressure dependence of the melting point has been discussed very widely. In the opinion of some workers,<sup>[8,9]</sup> the fusion curves should end at the critical points. Moreover, it has been suggested that the fusion curves should rise to a certain temperature maximum and then decrease. In such cases, we may find that, at sufficiently high temperatures, not even the highest pressures will be able to make a substance crystalline.<sup>[10]</sup>

Bridgman concluded from his own experimental data that the normal form of the fusion curve was a monotonic rise with pressure.<sup>[11]</sup> This dependence is described satisfactorily by Simon's equation in the form

$$P \div P_0 = bT^c,$$

where  $b$  and  $c$  are constants and  $P_0$  is the internal

pressure which must be overcome to melt a solid at absolute zero.<sup>[12,13]</sup>

Bridgman's view was the accepted one for a very long time but, recently, considerable experimental data have been collected over a wider range of pressures. In considering the  $P$ - $T$  diagrams of various elements, we can see that the negative slope of the fusion curve can no longer be regarded as anomalous: it is as normal as the positive slope. Simon's equation is valid only at low pressures and invalid in those cases when the fusion curve has negative slope (as observed in bismuth, antimony, gallium, silicon, germanium, and other elements), or if it passes through a maximum (cesium, barium, or tellurium) or a minimum (cerium).

Evidently, the monotonic nature of the fusion curve is a property of those elements whose atomic packing is not changed by pressure in the solid or liquid phases.

A general tendency in the sequence of polymorphic modifications of elements, observed as the pressure is increased, is the transition to more closely packed and more ordered structures. Such transitions are accompanied by an increase in the coordination number and an increase in the packing factor. Very frequently elements in a given group have the same sequence of polymorphic changes in the crystal structure when the pressure is increased. In some groups—for example, IV-B, V-B—this sequence is identical with the sequence of changes in the crystal structure when one element is transformed into another within the group. These tendencies are closely related to the similarity of the  $P$ - $T$  phase diagrams and, together with the latter, may be used as the basis for predictions of crystal structures not yet investigated or high-pressure modifications which are difficult to produce.

X-ray high-pressure cameras of various constructions are used in high-pressure technique to study the structures of polymorphic modifications.<sup>[14-19]</sup> They are all based on the use of high-pressure chambers made of materials which are relatively transparent to x-rays; in most cases, amorphous boron, beryllium, or diamond is used to make the high-pressure chamber of an x-ray camera. X rays are scattered both in the investigated substance and in the high-pressure chamber, which increases the general background in the x-ray-diffraction patterns and leads to the loss of a number of reflections for a given sample, particularly the low-intensity reflections. X-ray exposure in high-pressure chambers also meets with other problems (which will not be discussed here) all of which make the x-ray-diffraction analysis under pressure one of the most difficult physical experiments. These difficulties explain the absence of structure data for many of the known high-pressure polymorphic modifications of various substances.

In view of this, it becomes obvious how important are well-founded predictions of crystal structures of high-pressure phases. We shall now consider the poly-

\*This review of the  $P$ - $T$  phase diagrams covers work published up to May, 1965.

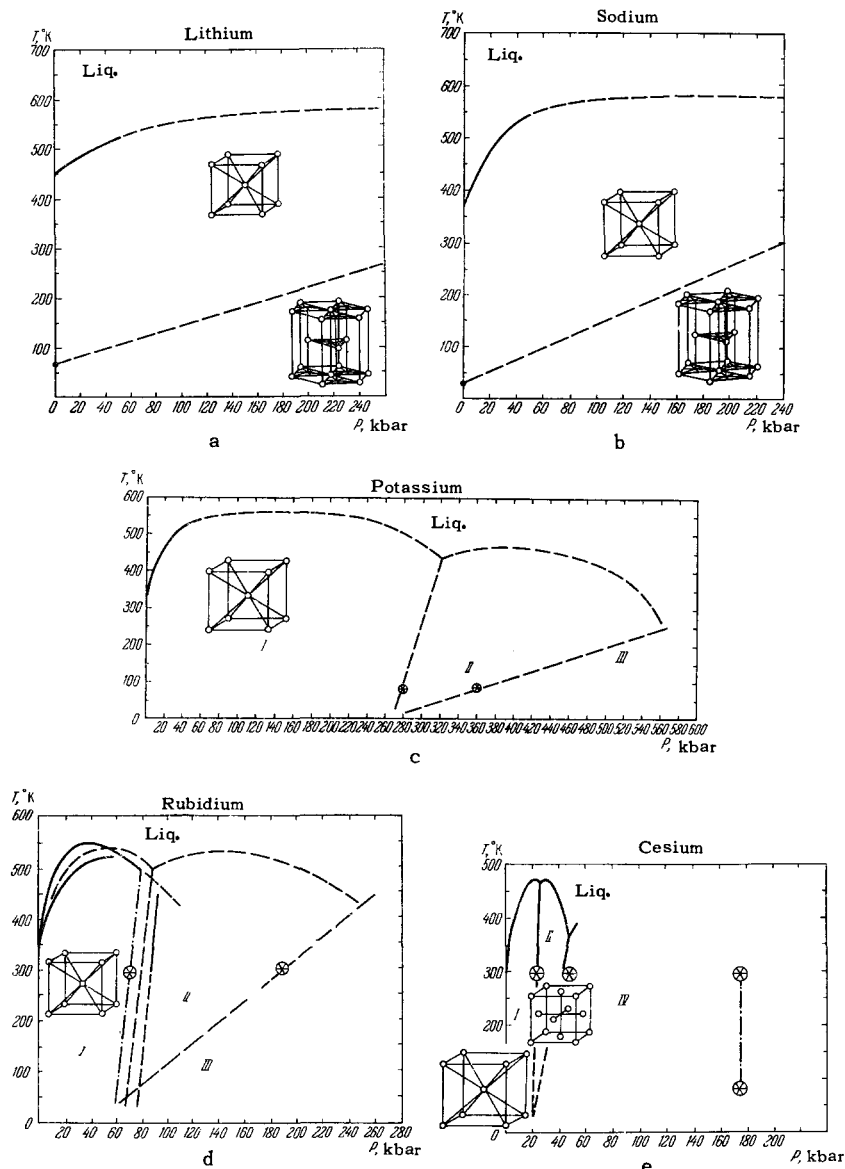


FIG. 1. P-T phase diagrams of Li, Na, K, Rb, and Cs. The fusion curves were obtained by the DTA method in [27]. The points on the ordinate in the Li and Na diagrams represent the polymorphic transition temperatures,<sup>[29]</sup> and the "stars" in all the diagrams represent the coordinates of the polymorphic transitions, found from electrical resistance discontinuities.<sup>[28]</sup> The upper fusion curve of Rb and a part of the phase boundary between RbI and RbII, shown by continuous lines, were obtained from electrical resistance discontinuities.<sup>[30]</sup> The Cs diagram up to 60 kbar was obtained by the DTA method<sup>[23]</sup> and the polymorphic transitions at 175 kbar were found from electrical resistance discontinuities.<sup>[24]</sup> In these and later diagrams, the hypothetical phase boundaries are shown dashed.

morphism of elements in the periodic system using the available information.

## 2. ALKALI METALS OF GROUP I-A

Normally, all alkali metals have the bcc lattice of type A2, \* with a packing factor (which is the ratio of the volume occupied by atoms to the total volume of a cell)  $\varphi = 0.68$ . When cooled under pressure, the crystal structure of these metals changes. This can be seen clearly in their P-T phase diagrams, which are shown in Fig. 1.

In the pressure range up to 60 kbar<sup>†</sup>, the most well defined among the P-T diagrams is that of cesium. While investigating the specific volume of cesium and

its electrical resistance as a function of pressure, Bridgman established the existence of two polymorphic transitions, at 23 and 45 kbar.<sup>[20,21]</sup> Particularly important were the results found for the transition at 45 kbar, because this transition was accompanied by a surprisingly large discontinuity in the volume (12%) and a change in the electrical resistance of an unusual type—the curve had a peak. Consequently, cesium has become the subject of a host of investigations; it was recently shown that the pressure dependence of the electrical resistance of cesium was more likely to be a sharp peak with a small plateau at its apex.<sup>[22]</sup>

Figure 2 shows this dependence, together with the curve found by Bridgman. This form of pressure dependence suggested that another modification of cesium, Cs III, existed over a very narrow range of pressures (0.5 kbar only).

The P-T phase diagram of cesium was determined to 60 kbar and showed boundaries between the regions of stability of three modifications: Cs I, Cs II, and

\*Here and later, we shall use the structure notation proposed in "Strukturbericht." A2 is a bcc cube of the tungsten type.

<sup>†</sup>1 bar =  $10^6$  dyn/cm<sup>2</sup> = 1.0197 kg/cm<sup>2</sup> = 0.98692 normal atmospheres.

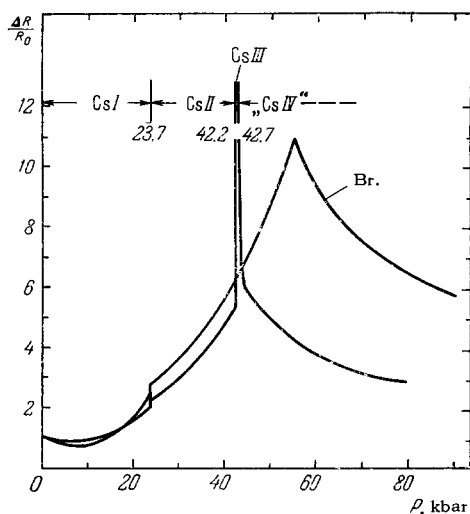


FIG. 2. Dependence of the electrical resistance of Cs on pressure.<sup>[22]</sup> The pressure scale should be corrected for Bridgman's curve (Br):<sup>[31]</sup> 100 kbar on the old scale corresponds to 80 kbar on the new scale.

Cs IV.<sup>[23]</sup> The chain curve in the region of 175 kbar in Fig. 1e shows part of the boundary between the high-pressure phases, found from the electrical resistance discontinuities and reported in<sup>[24]</sup>.

X-ray-structure analysis under pressure was used to determine the crystal structures of the modifications Cs II and Cs III.<sup>[22]</sup> It was found that the initially bcc lattice was transformed under pressure into a more closely packed lattice: the fcc lattice of the copper type (type A1) with a lattice constant  $a = 5.984 \pm 0.01 \text{ \AA}$  (at 41 kbar). Further increase in pressure produced a new modification at 42.4 kbar, with the same crystal structure (fcc type A1) but with a smaller lattice parameter:  $a = 5.800 \pm 0.007 \text{ \AA}$  (at 42.5 kbar). Calculations showed that an isomorphous transition in cesium in which the crystal structure was retained could have been the result of an internal rearrangement within the atoms, i.e., the result of a transition of the valence electrons from the 6s- to the 5d-state.<sup>[5,32]</sup>

An electronic transition accompanied by the isomorphous A1  $\rightarrow$  A1 transformation has been found in one other element: the rare-earth cerium, in which pressure produces an electronic transition from the 4f- to the 5d-state.

Debye diffraction patterns of the Cs IV modification were reported also in<sup>[22]</sup>, but in this case it was not possible to index reliably the diffraction reflections. The patterns obtained suggested that this modification had stacking faults or an hcp structure with twin c-axes, similar to that observed in rare-earths of the lanthanum type (type A3').

In connection with this, it should be mentioned that the fcc type A1 structure, the hcp magnesium type (A3) structure, and the lanthanum (A3') structure are all very similar in their packing of the layers. This

can be understood by considering Figs. 3 and 4, which show unit cells for these three structures. Thus, the high-pressure modification Cs IV is very likely to have the hcp type A3 structure.

Rubidium has physical and chemical properties which are very similar to those of cesium and it may have a P-T phase diagram similar to that of cesium. If this is correct, the rubidium diagram should have a form close to that shown in Fig. 1d. The same is true of potassium: so far, we know only a part of its fusion curve up to 60 kbar<sup>[27]</sup> and two points at which electrical resistance discontinuities have been observed.<sup>[28]</sup> Here and later, we shall use dashed curves to denote probable phase boundaries.

Lithium and sodium probably have simpler diagrams due to the simpler structure of their atoms. The boundary between phases I and II of lithium and sodium intersects the temperature axis, and the low-temperature phase has been investigated at atmospheric pressure. X-ray diffraction analysis showed that after a polymorphic transition, these metals had the hcp type A3 lattice, similar to that of magnesium.<sup>[29]</sup>

Compared with the initial bcc structure, the A3 lattice is more compact with a packing factor  $\varphi = 0.74$ .

### 3. ALKALINE-EARTH METALS OF GROUP II-A

We shall consider the elements of group II-A in the

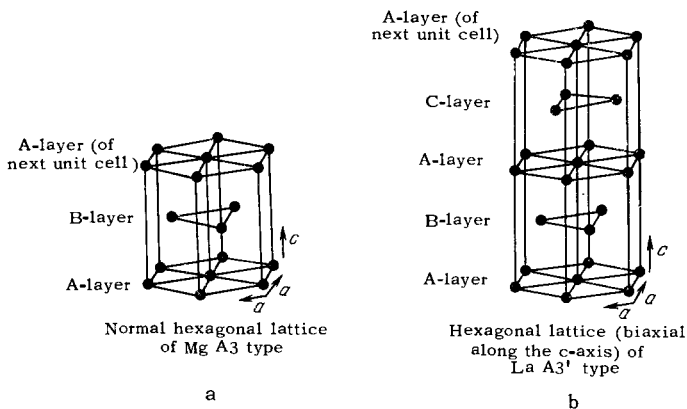


FIG. 3. Distribution of atoms in hcp structures of the Mg A3 type (a) and of the La A3' type (b).

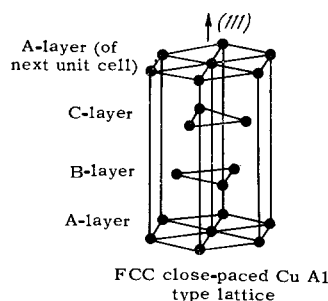


FIG. 4. Distribution of atoms in the fcc Cu A1 type structure. Unit cell is shown in hexagonal axes.

same sequence as in the periodic table. Under normal conditions, metallic beryllium crystallizes, like its neighbor magnesium, in the hcp type A3 lattice. We must mention that two more elements—zinc and cadmium—in group II have a similar lattice and if the ideal ratio of axes for this type of structure is  $c/a = 1.63$ , then beryllium and magnesium have unit cells flattened along the  $c$ -axis, while zinc and cadmium have unit cells elongated along this axis.

Beryllium exhibits a somewhat unusual high-temperature polymorphism: at 1254°C, its crystal structure changes to the bcc type A2,<sup>[33]</sup> and the high-temperature phase has a higher density. This phase is probably stable also at high pressures. If this is correct, then the boundary between the two phases with the structures A3 and A2 should have a negative slope intersecting, at room temperature, the pressure axis in the region of 93 kbar, where a strong discontinuity of the electrical resistance, ascribed to a polymorphic transition, was observed.<sup>[34]</sup>

Magnesium does not exhibit polymorphism when the temperature or pressure is increased. The electrical resistance of magnesium varies monotonically with pressure up to 500 kbar, exhibiting only several weak maxima and minima.<sup>[35]</sup> The fusion curves of magnesium and beryllium are not yet known.

The  $P$ - $T$  phase diagrams of calcium and strontium were obtained up to 40 kbar;<sup>[36]</sup> they are shown in Figs. 5a and 5b. Under normal conditions, these metals crystallize in the fcc type A1 lattice but on heating they undergo a polymorphic transition with a change in structure to the bcc type A2. From the phase diagrams,

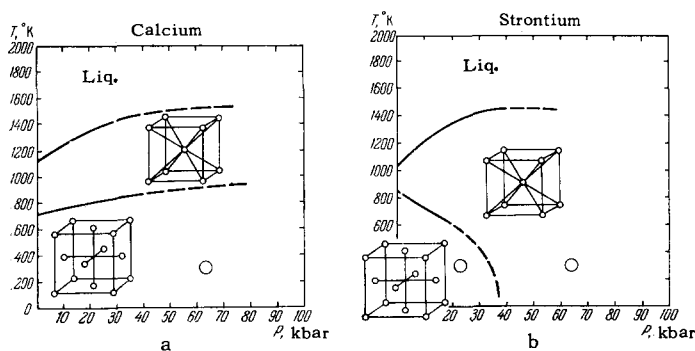


FIG. 5.  $P$ - $T$  diagrams of Ca and Sr (according to DTA data<sup>[36]</sup>). Circles denote conditions under which Bridgman observed volume discontinuities.<sup>[37]</sup>

it follows that the high-temperature phases of these elements are stable also at high pressures. It should be mentioned that highly impure samples of these metals exhibited stable phases with the hexagonal type A3 structure, but the purification of Ca and Sr established that in their pure form these metals had only the two phases mentioned above.<sup>[38]</sup> The volume discontinuities observed in calcium and strontium by Bridgman (denoted by circles in the  $P$ - $T$  diagrams) were prob-

ably due to impurities. X-ray diffraction analysis of the high-pressure phase of strontium, carried out at 40 kbar and room temperature, showed definitely that the structure was identical with the high-temperature modification.<sup>[39]</sup> The identity of the pressure dependences of the electrical resistance of strontium and calcium allows us to assume that the transitions at 35 kbar in strontium and at 375 kbar in calcium<sup>[35]</sup> have the same nature; these dependences are shown in Figs. 6 and 7. The boundary between the solid phases of calcium is initially parallel to the fusion curves and then it turns in the direction of the pressure axis, passes through the coordinate  $P = 375$  kbar,  $T = 20^\circ\text{C}$  and intersects the pressure axis in the region of absolute zero, making a right-angle with this axis. In this case, as in the case of alkali metals, the  $P$ - $T$  diagram of strontium is the "compressed" variant of the  $P$ - $T$  diagram of its immediate neighbor, calcium.

Metallic barium has properties very similar to those of elements of groups I-A and it crystallizes, under normal conditions, in the bcc form. Its  $P$ - $T$  phase diagram, shown in Fig. 8, is also very similar to the  $P$ - $T$  diagrams of alkali metals. The phase diagram of barium is plotted on the basis of data taken from several papers: the fusion curve up to 70 kbar was found by the differential thermal analysis (DTA) method, but the data were contradictory for the boundary between the solid phases Ba I and Ba II. The differential thermal analysis gave a boundary with a positive slope<sup>[40]</sup> and the method of electrical resistance discontinuities gave a phase boundary with a negative slope.<sup>[41]</sup> Dash-dot

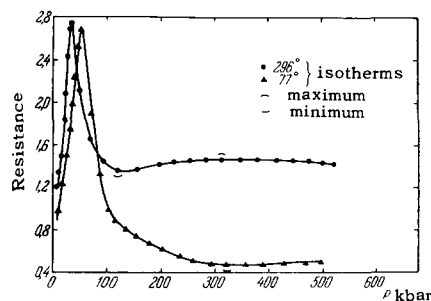


FIG. 6. Dependence of the electrical resistance of Sr on pressure.<sup>[35]</sup>

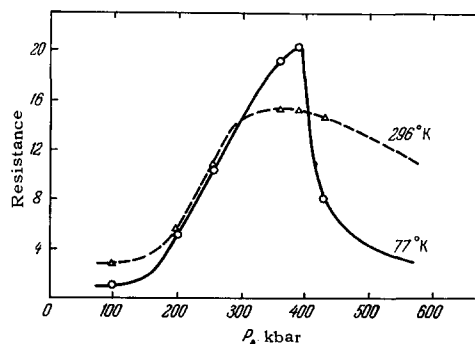


FIG. 7. Dependence of the electrical resistance of Ca on pressure.<sup>[35]</sup>

curves are used for the fusion curve and the Ba I–Ba II phase boundary in Fig. 8, plotted using these data. The continuation of the fusion curve and the Ba II–Ba III phase boundary in the pressure region from 140 to 400 kbar was also found from the electrical resistance discontinuities.<sup>[35]</sup> A part of the boundary between the solid phases in the 15–20 kbar region was obtained by Bridgman from measurements of the volume discontinuity at a polymorphic transition.<sup>[42]</sup> X-ray diffraction analysis carried out at room temperature up to pressures of 60 kbar showed no changes in the structure up to 59 kbar and then the diffraction pattern changed, accompanied by a sharp increase in the electrical resistance.<sup>[43]</sup> The x-ray structure analysis data showed that the Ba II modification had the hcp A3 type structure.

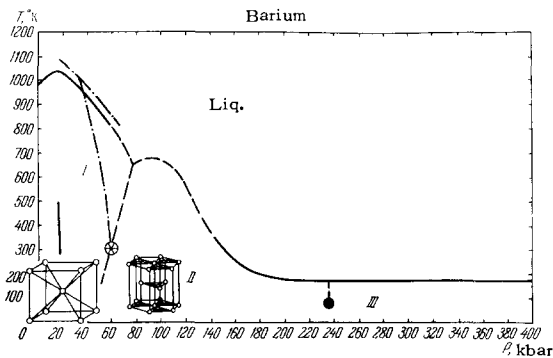


FIG. 8. P–T phase diagram of Ba. The fusion curve and a part of the phase boundary in the region of 60 kbar, shown by continuous lines, are plotted in accordance with the DTA method.<sup>[40]</sup> A part of the boundary in the 15–20 kbar region was found by Bridgman from volume discontinuities.<sup>[42]</sup> Dot-dash curves indicate the fusion curve and the phase boundary found from resistance discontinuities;<sup>[41]</sup> the same method was employed to find the part of the diagram between 140 and 400 kbar.<sup>[35]</sup>

#### 4. METALS OF GROUP II-B

As mentioned before, zinc and cadmium have hcp type A3 structure, strongly elongated along the c axis. The ratio of the axes is  $c/a = 1.86$  for zinc and  $c/a = 1.89$  for cadmium, i.e., the interatomic bonds in the hexagonal layers are stronger than along the c axis between the layers. In the case of mercury, the binding forces in the crystal lattice are even weaker and under normal conditions it is liquid. When it solidifies, mercury crystallizes in the  $\alpha$ -modification with the orthorhombic type A10 lattice with a single atom per unit cell. This structure can also be described in terms of hexagonal axes; it is then found that the ratio of the axes is  $c/a = 1.94$ .

Thus, metals of group II-B have a very loose structure with strongly anisotropic physical properties; for example, the compressibility of cadmium along the c axis is seven times higher than its compressibility along the a axis.

Polymorphism has not been observed in polycrystal-

line samples of cadmium and zinc at pressures up to 100 kbar.<sup>[37]</sup> However, Bridgman found that cadmium single crystals exhibited a clear volume discontinuity in the region up to 10 kbar;<sup>[44]</sup> he also plotted parts of the phase boundaries, assuming the existence of polymorphic transitions. In the phase diagram of cadmium, shown in Fig. 9b, the Bridgman data are in the form of short lines in the region of 10 kbar. X-ray diffraction analysis was carried out on polycrystalline cadmium but it revealed no changes in the structure at pressures up to 16 kbar;<sup>[46]</sup> it is possible that Bridgman observed the twinning of single crystals under pressure, especially as twinning is very easy in cadmium.<sup>[47]</sup>

The P–T phase diagram of mercury is shown in Fig. 10; it is clear that the boundary between the solid phases  $\alpha$  and  $\beta$  is almost parallel to the fusion curve.

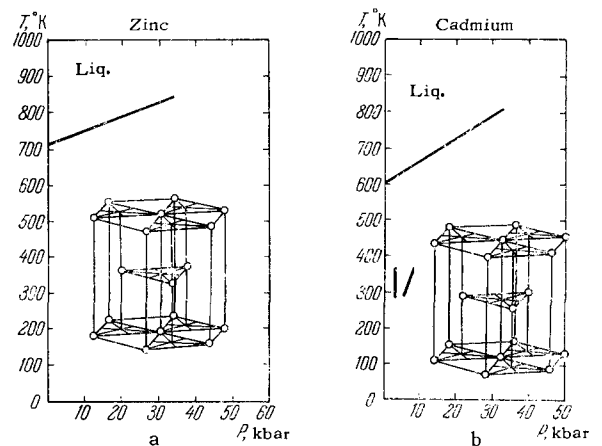


FIG. 9. P–T diagrams of Zn and Cd. The fusion curves were obtained by the DTA method.<sup>[45]</sup> The parts of the boundaries between the solid Cd phases were found from volume discontinuities in single crystals.<sup>[44]</sup>

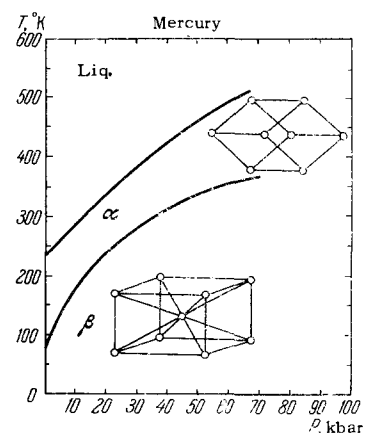


FIG. 10. P–T phase diagram of Hg.<sup>[48]</sup>

Since the  $\beta$ -Hg modification is stable at low temperatures and atmospheric pressure, it was investigated using the low-temperature x-ray diffraction technique.<sup>[49]</sup> The analysis showed that the high-pressure phase  $\beta$ -Hg had the tetragonal body-centered structure with two

atoms per unit cell and the axis ratio  $c/a = 0.706$ . In this structure, each atom has two nearest neighbors along the  $c$  axis and, therefore, the atoms are linked into narrow rows elongated along this axis. Investigations of the electrical resistance showed no polymorphism in the  $\beta$ -modification of mercury up to 100 kbar. [37]

## 5. RARE-EARTH ELEMENTS

Rare-earth elements are distinguished by a great similarity of their physical and chemical properties—a consequence of their electron structure. Usually, these metals are divided into two subgroups: cerium (from Ce to Gd) and yttrium (from Tb to Lu); within these subgroups, the properties of the lanthanides show even greater similarity. We shall consider only one of these properties, i.e., polymorphism.

Under normal conditions, all elements in the yttrium subgroup crystallize in the hcp magnesium (type A3) structure with the axis ratio  $c/a = 1.6$ . The only exception is ytterbium, which has the fcc lattice.

The elements in the cerium subgroup exhibit an even greater variety of crystal structures.  $\alpha$ -lanthanum,  $\alpha$ -praseodymium, and  $\alpha$ -neodymium have the hcp lanthanum-type A3' lattice with  $c/a = 3.2$ . This structure is characterized by an alternate packing layers of the ABACA... type. Samarium also has the hcp lattice but with a different sequence of layers—ABABCBCACA...—and the ratio  $c/a = 7.25$ ; however, the true structure of samarium is rhombohedral. Metallic cerium, under normal conditions, has two phases: one of them is  $\gamma$ -cerium with an fcc lattice, and the other is the metastable  $\beta$ -cerium phase with the hcp type A3 lattice, whose range of stability in the  $P$ - $T$  diagram has not yet been determined. Europium has a bcc lattice.

Most lanthanides, with very few exceptions, are now known to exhibit the temperature polymorphism and all high-temperature modifications have the bcc structure. Many lanthanides also exhibit polymorphism under the action of high pressures. Lanthanides have similar properties and are very likely to have similar polymorphism and display great similarity in the  $P$ - $T$  diagrams. Unfortunately, only very few data are available on the  $P$ - $T$  diagrams of rare earths.

Figure 11 shows the  $P$ - $T$  diagram of cerium. The  $\gamma \rightarrow \alpha$  transition in cerium is one of the most remarkable because it is an isomorphous transition; at room temperature, it is accompanied by a considerable sudden change in volume, while the structure of the high-pressure modification remains, as before, fcc. [4]

The reverse  $\alpha \rightarrow \gamma$  transition takes place when the pressure is reduced after some delay (hysteresis) but this hysteresis decreases when the temperature is increased. The values of  $\Delta V$  (volume discontinuity at transition) and  $\Delta Q$  (heat of transition) both decrease as well. This has suggested that the phase boundary between the  $\alpha$ - and  $\gamma$ -modifications ends at the criti-

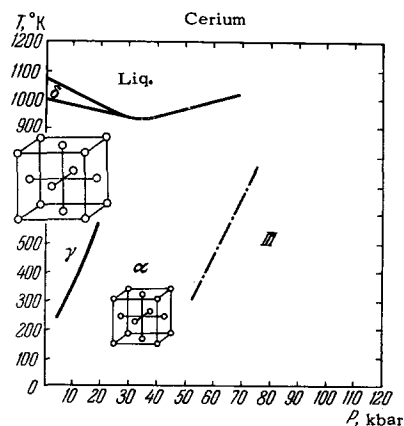


FIG. 11.  $P$ - $T$  phase diagram of Ce. [51, 53] The  $\gamma \rightarrow \alpha$  boundary was obtained by the volume discontinuity method; the probable boundary between the  $\alpha$ - and Ce-III phases (dash-dot line) was obtained from the pressure dependence of the electrical resistance.

cal point with the coordinates  $280^\circ\text{C}$ ,  $18.5 \text{ kg/cm}^2$ . [50] It must be mentioned that somewhat later an increase in the experimental accuracy made it possible to extend the phase boundary to the coordinate  $400^\circ\text{C}$ ,  $20 \text{ kg/cm}^2$  and it was suggested that this boundary met the fusion curve. [5] However, recent x-ray investigations showed that the (111) reflections of both phases converged as the temperature was increased along the phase boundary. Extrapolation to the point of convergence of the two phases, i.e., to the parameters of a possible critical point, gave the values  $350$ – $400^\circ\text{C}$  and  $20$ – $22 \text{ kbar}$ . [52]

In the  $\alpha \rightarrow \gamma$  transition in cerium, we have, so far, the only example of a boundary between two solid phases ending at a critical point.

It is interesting to note that the extrapolation of the phase boundary leads, in this case, to a broad minimum in the fusion curve, which has been found only in cerium.

The chain curve in Fig. 11 represents the boundary between the phases  $\alpha$  and Ce-III; it was found from irregularities in the pressure dependence of the electrical resistance of cerium. [51] We may assume that the structure of the Ce-III modification is compact, most likely hcp.

Lanthanum, praseodymium, and neodymium have very similar properties. As mentioned before, under normal conditions, they have the lanthanum type A3' structure, which is hcp with the ratio  $c/a = 3.2$ , i.e., approximately twice as large as for normal metals having the type A3 lattice. On heating, the type A3' lattice is replaced by a bcc lattice, as is frequently observed in metals. At atmospheric pressure, lanthanum has one more modification,  $\beta$ -La, which has the fcc type A1 structure. The high-temperature modification, as indicated in the  $P$ - $T$  phase diagram in Fig. 12a, is also stable at high pressures. Investigation of its crystal structure confirmed once again the

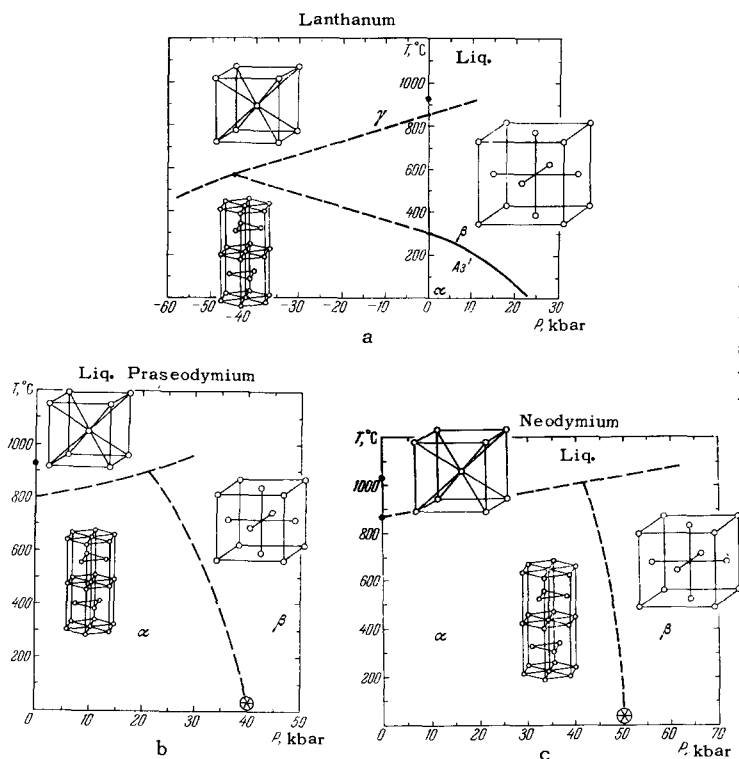


FIG. 12. The P-T diagrams of La, Pr, and Nd. The boundary between the  $\alpha$ - and  $\beta$ -phases of lanthanum was found from electrical resistance discontinuities.<sup>[54]</sup> The P-T diagrams of Pr and Nd are hypothetical. The only reliable features are  $T_{m,p}$ , the  $\alpha \rightarrow \gamma$  transition temperatures, and the coordinates of the transition from the  $\alpha$ -phase to the high-pressure phase.<sup>[55]</sup>

identity of the high-temperature phase with the high-pressure phase and showed that the lanthanum type structure (A3') changed under pressure into the fcc type A1 structure.<sup>[55]</sup>

Exactly the same polymorphism is exhibited by the neighbors of lanthanum—praseodymium and neodymium. The polymorphism of praseodymium was established earlier from the discontinuity in the shear stress<sup>[56]</sup> and from the discontinuity in the electrical resistance<sup>[21]</sup> at 50 kbar, but no anomalies were found in the properties of neodymium up to 100 kbar.<sup>[20]</sup> X-ray diffraction established clearly that, in both these metals, the crystal structure changed from A3' to A1, as in lanthanum.<sup>[55]</sup> Unfortunately, the P-T diagrams for these metals are not available but it seems very likely that these close analogs of lanthanum have P-T diagrams very similar to the diagram of lanthanum. These hypothetical diagrams, with phase boundaries shown by dashed curves, are given in Figs. 12b and 12c. It is very likely that the negative slope between the phases A3' and A1 is retained but it may vary from element to element, and, therefore, while the triple point between the phases A3', A2, and A1 of lanthanum is in the range of negative pressures, the analogous triple points of Pr and Nd should be in the range of real pressures, and in the case of Nd the triple point should be at high pressures. This form of the P-T diagram may explain why no fcc modification is observed in praseodymium and neodymium at atmospheric pressure.

The question now arises whether these metals have an isotropic transition, similar to that observed in cerium at a pressure of only 7 kbar and accompanied

by a rearrangement of the type A1 lattice into a flattened fcc lattice. So far, there are no data to confirm this hypothesis but the existence of such a transition in La, Pr, and Nd seems very likely.

Recently, reports have been published on polymorphism under pressure in gadolinium<sup>[57]</sup> and samarium.<sup>[58]</sup> As mentioned earlier, under normal conditions, samarium has a remarkable crystal structure. If it is considered in terms of a hexagonal axis, its unit cell is very much elongated along the c axis; it is filled with atoms in ten consecutive layers. A new phase was found at 40 kbar and 300°C<sup>[58]</sup>, which was retained in the metastable state even after the removal of pressure, and was investigated by x-ray diffraction. Analysis of the Debye diffraction pattern showed that the new phase had the hcp lanthanum A3' structure.

However, the problem of the stability of this modification of samarium under pressure will be resolved finally only when x-ray analysis is carried out at 40 kbar and 300°C. The point is that metastable forms of various elements may exist under conditions which are far from their stability zone. For example, the metastable phases of carbon<sup>[59]</sup> or silicon<sup>[60]</sup> exhibit complex crystal structures; the stability zones of these phases have not yet been found in the P-T phase diagrams of carbon and silicon.

The same applies to gadolinium; a metastable form was obtained at 40 kbar and 400°C. X-ray diffraction analysis showed that the new phase had the samarium-type structure but there were also traces of a phase with the lanthanum type A3' structure.<sup>[57]</sup>

Bridgman found both volume discontinuities and anomalies in the electrical resistance of gadolinium



at pressures of 20–25 kbar.<sup>[61]</sup> However, it is not clear at all that the metastable phase of gadolinium is formed at this transition. The following suggestion has been made for the sequence of changes in the crystal structure of rare-earth metals during polymorphic transitions under pressure: hcp (type A3) → samarium type → lanthanum (A3') type → fcc (type A1). To confirm or reject this scheme, we would need to carry out x-ray analyses at high pressures.

The rare earths europium and ytterbium are very similar to alkaline-earth metals; this applies both to their chemical activity (they are divalent) and such physical properties as the crystal structure, volatility, refractory properties, thermal expansion, and compressibility.

The similarity of the properties of europium and ytterbium to the properties of alkaline-earth metals is explained by the stability of the half-filled and completely-filled 4f-states of these elements. Their P-T phase diagrams (Figs. 13 and 14) are very similar to the diagrams of alkaline-earth metals.

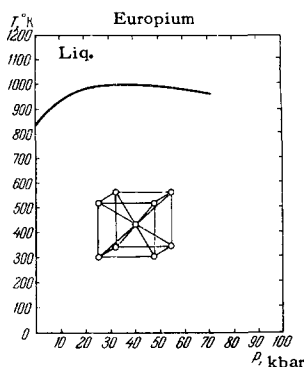


FIG. 13. P-T diagram of Eu (according to the DTA method<sup>[65]</sup>).

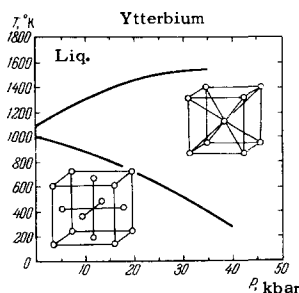


FIG. 14. P-T phase diagram of Yb (according to the DTA method<sup>[63]</sup>).

Europium has a fusion curve with a clear maximum, similar to that observed for barium. Like the alkaline-earth barium, europium crystallizes in the bcc type A2 structure. It is assumed that the electrical resistance discontinuity, which is observed in europium at 150–160 kbar,<sup>[62]</sup> is due to a polymorphic transition with a change in the bcc lattice to the hcp type A3 lattice, i.e., due to the same structure change as in barium at 59 kbar.<sup>[63]</sup>

Since the similarity between these two metals is so great, it seems possible that there is an A2 → A2 transition in europium at a pressure of the order of 30 kbar, similar to that which occurs in barium at 17 kbar.

The rare-earth ytterbium has properties which resemble most those of the alkaline-earth strontium and, as can be seen from Figs. 6 and 14, the P-T phase diagram of this element is very similar to the diagram for strontium.<sup>[63]</sup> Under normal conditions, both strontium and ytterbium crystallize in the fcc type A1 lattice, which changes, when the temperature is increased, to a bcc lattice. The P-T diagrams show that the boundary between the  $\alpha$ - and  $\beta$ -phases of these elements has a negative slope and that the high-temperature phase is stable also at high pressures. X-ray structure analysis carried out at high pressures definitely confirmed the complete identity of the high-temperature and high-pressure modifications.<sup>[64]</sup>

## 6. METALS OF GROUP III-B

In spite of the fact that fairly complete P-T diagrams are available for group III-B metals up to 70 kbar, this group is most difficult as far as generalizations are concerned. We shall show below that it is natural to consider together aluminum, gallium and indium, and, separately, thallium.

Under normal conditions, aluminum has the type A1 fcc lattice and does not exhibit polymorphism under pressure or when the temperature is increased. This metal exhibits considerable electrical conductivity, which is slightly and monotonically increased by pressures up to 100 kbar.<sup>[20]</sup> The fusion curve of aluminum, found by differential thermal analysis,<sup>[65]</sup> is shown in Fig. 15a.

Gallium has three modifications in the pressure range up to 100 kbar; its P-T diagram is shown in Fig. 15b. The low-pressure phase has an orthorhombic structure with eight atoms in a unit cell. Each atom in this structure has only one nearest neighbor [the coordination number (c.n.) is 1], i.e., atoms are arranged in pairs—"molecules." The binding between such pairs in the lattice is quite weak and a metal having this structure has a low melting point. When the pressure is increased, the crystal structure changes to the Ga II modification, which, as shown by x-ray structure analysis under pressure,<sup>[66]</sup> has the tetragonal face-centered lattice (c.n. = 4.8) with a very small difference between the c- and a-axes, so that the ratio of the axes is  $c/a = 1.104$  at 30 kbar; it is worth noting that metallic indium has the same structure (type A6) under normal conditions.

It has been suggested<sup>[65]</sup> that the structure of Ga III is the bcc type A2; this hypothesis is very likely to be true since the great majority of high-temperature phases of metals is of this structure. It seems to us that there is another possibility—the structure may be the fcc type A1 because the tetragonal structure of indium differs so little from the fcc structure, that it can assume the latter form under pressure. The tetragonal fcc lattice of indium (type A6, 4 atoms/cell, c.n. = 4) has an even smaller difference between the axes under normal conditions  $c/a = 1.077$ .

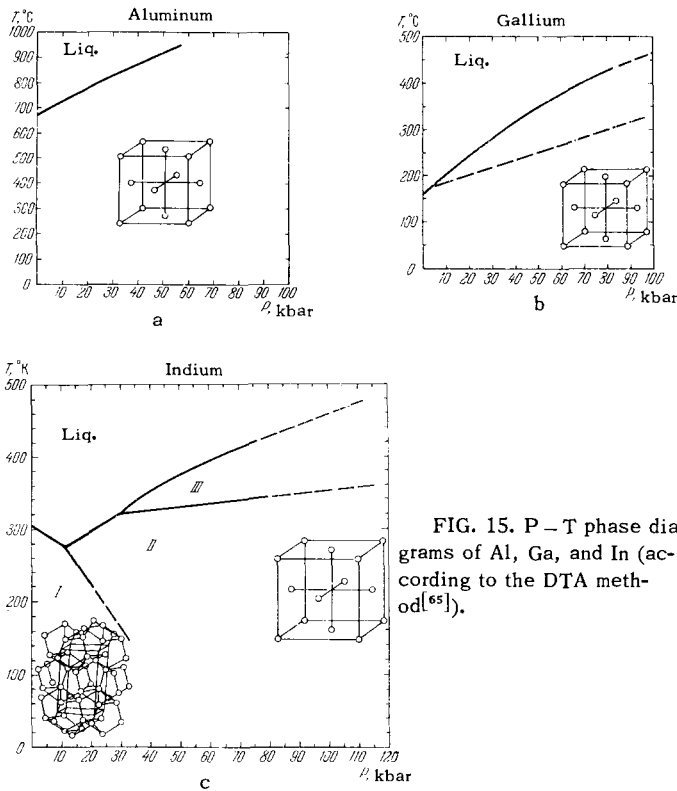


FIG. 15. P-T phase diagrams of Al, Ga, and In (according to the DTA method<sup>[65]</sup>).

The A6 → A1 transition, as shown by x-ray-structure analysis, occurs in metallic indium at atmospheric pressure when the temperature is increased.<sup>[67]</sup> It would seem, therefore, that the boundary between the solid phases should be that indicated by the dashed line in Fig. 15c. It is, at present, impossible to find the point where this line intersects the fusion curve.

Thus, considering elements of group III-B, we can see their general tendency to have fcc structures.

Thallium, which follows indium in this subgroup, has a P-T diagram (Fig. 16) different from the diagrams of its neighbors in the same group but resembling strongly the P-T diagrams of zirconium and titanium.

It is evident from this diagram that, in the region up to 60 kbar, thallium has three modifications. The phase stable under normal conditions has the hcp type A3 structure, while the high-temperature phase has a bcc structure. As in the case of titanium and zirco-

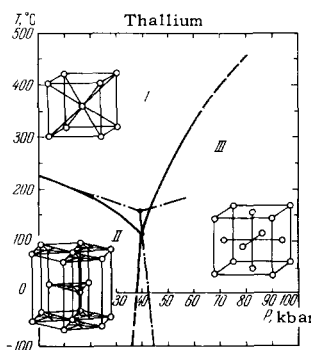


FIG. 16. P-T phase diagram of Tl (according to the DTA method<sup>[65]</sup>). Dash-dot lines show the boundaries between phases found by Bridgman using the volume discontinuity method.<sup>[68]</sup>

mium, the high-temperature phase of thallium has a higher density than the low-temperature phase, i.e., as the temperature is increased, there is a polymorphic transition with a negative change in volume—the specific volume per atom decreases.

Pressure reduces the temperature of the A3 → A2 transition; the boundary between these two phases has a negative slope. As the pressure is further increased, these two phases change; the atoms become rearranged to form an fcc lattice. The possible structure of the Tl III phase was discussed in <sup>[69]</sup> on the basis of thermodynamic data and in <sup>[70]</sup> by invoking the concept of the spatial packing of atoms; the authors of both papers concluded that this modification had the fcc type A1 lattice structure. X-ray-structure analysis of this phase under pressure confirmed this conclusion.<sup>[16]</sup>

### 7. METALS OF GROUP IV-A

Titanium, zirconium, and hafnium exhibit polymorphism of a very special type. Their  $\alpha$ -phases with the hcp type A3 lattice, which exist under normal conditions, change to the  $\beta$ -form when the temperature is increased and into the  $\omega$ -form when the pressure is increased. The differential thermal analysis of titanium and zirconium established the boundaries between the  $\alpha$ - and  $\beta$ -modifications and, in the case of zirconium, parts of the boundary between the high-pressure  $\omega$  phase and the  $\alpha$ - and  $\beta$ -modifications were also determined. Figure 17a shows the P-T diagram of titanium, and Fig. 17b the P-T diagram of zirconium (in accordance with <sup>[71]</sup>).

The high-temperature  $\beta$ -phases of these metals have a bcc structure, like the majority of metals. However, all the transitions referred to are anomalous since they are accompanied by volume discontinuities and the high-temperature  $\beta$ -modification has a higher density than the  $\alpha$ -phase.

This observation suggests that the high-pressure phase may have the same structure. The same conclusion was reached by considering the high-pressure phase on the basis of thermodynamic data.<sup>[72]</sup> In fact, x-ray structure analysis of these metals, carried out at pressures higher than the transition pressure, showed that the high-pressure phases of titanium and zirconium had a bcc structure.<sup>[73]</sup> The high-pressure phase of titanium and zirconium was called the  $\omega$ -phase by analogy with the structure found in titanium and zirconium alloys.<sup>[74,75]</sup> The high-temperature  $\beta$ -phase and the high-pressure  $\omega$ -phase of these metals are not identical but they may be regarded as isomorphous. As proved for zirconium, the transition between these phases occurs without a change in volume and has no hysteresis; the boundary between the phases is parallel to the pressure axis. It is possible that in the case of titanium the boundary between the analogous phases is also parallel to the pressure axis.

Thus, we may say that the phase diagrams of tita-

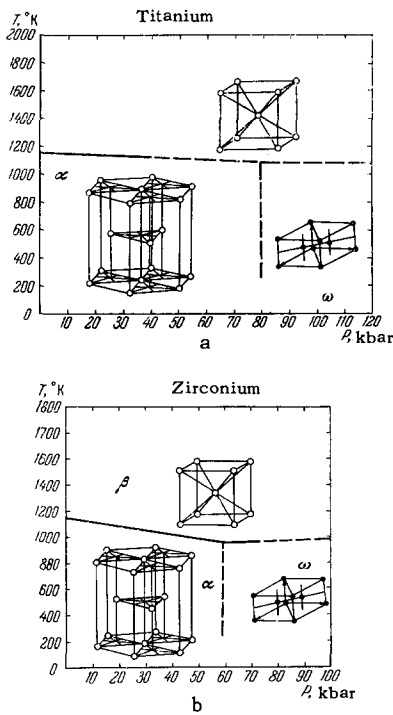


FIG. 17. Phase diagrams of Ti and Zr (according to the DTA method<sup>[71]</sup>).

nium and zirconium have much in common and, although their fusion curves have not yet been determined (they lie at fairly high temperatures), they should be similar. In elements of this subgroup, the melting points and the  $\alpha$ - $\beta$  transition temperatures

increase, and the pressures of the  $\alpha$ - $\omega$  transitions decrease along the sequence from Ti to Hf. However, it should be mentioned that on the basis of this sequence, one would expect hafnium to exhibit polymorphism at pressures less than 60 kbar but no volume or electrical resistance discontinuities have been observed for this metal and the x-ray structure analysis under pressure showed no change in the structure. This point will be resolved when the boundaries between the polymorphic modifications of hafnium in the P-T field are determined.

## 8. ELEMENTS OF GROUP IV-B

Elements of the carbon group exhibit a gradual change in their physical properties with increasing atomic number: these properties change from metalloid in carbon, through semiconducting in silicon and germanium, to metallic in tin and lead, which are superconducting at low temperatures. The crystal structure also changes gradually from element to element. Under normal conditions, carbon has the hexagonal layered structure of graphite (type A9), whilst silicon and germanium have the cubic diamond (type A4) structure, white tin ( $\beta$ -Sn) has the tetragonal body-centered structure (type A5) and lead the fcc structure (type A1). This sequence of structures in the carbon group can be expressed symbolically by  $A9 \rightarrow A4 \rightarrow A5 \rightarrow A1$ . All elements of this group undergo polymorphic transitions when there is an increase in the pressure or a change in temperature. It is found that the high-pressure modifications exhibit the same sequence in

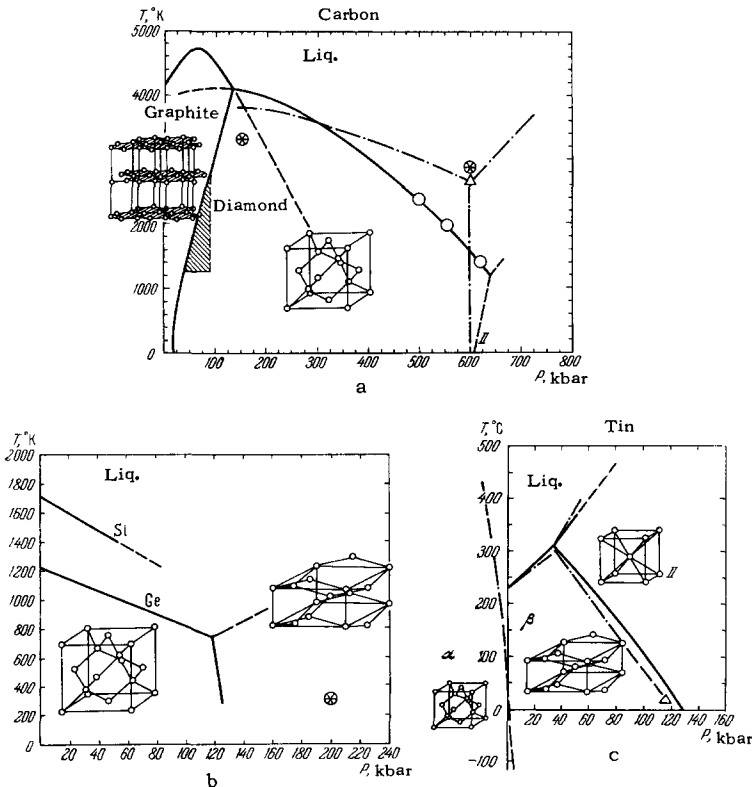


FIG. 18. a) P-T phase diagram of C.<sup>[76]</sup> The "stars" denote the triple points in the diagram reported in<sup>[77]</sup>; the circles denote the coordinates of the volume discontinuities obtained using shock waves.<sup>[78]</sup> The dash-dot lines show the phase boundaries and a triangle gives the triple point coordinates, all reported in<sup>[79]</sup>. The shaded zone is the region in which it is practical to produce synthetic diamonds. b) P-T diagrams of Si and Ge obtained by the DTA method.<sup>[79]</sup> A "star" denotes the conditions for a polymorphic transition in Si.<sup>[81]</sup> c) the P-T diagram of Sn was obtained by the DTA method<sup>[79]</sup> (shown by continuous curves); the dashed curves represent the  $\alpha$ - $\beta$  phase boundaries found by calculation;<sup>[79]</sup> chain curves are the boundaries found by x-ray structure analysis under pressure.<sup>[25]</sup>

the structures which is observed in the group as a whole in the transition from element to element. This can be easily understood if the P-T phase diagrams are considered in the same sequence.

Figure 18a shows, by continuous curves, the phase diagrams of carbon in accordance with [76]. The stable form of carbon under normal conditions is graphite and the metastable form is diamond. The boundary between these two phases, according to [76], intersects the fusion curve at 130 kbar and 4100°K, and the fusion curve of diamond has a considerable negative slope, so that the volume discontinuities in graphite, found by means of shock waves, [78] have been assumed to represent melting. The second triple point in the diagram (the point of intersection of the fusion curve with the boundary between the phases diamond and graphite-II) lies at 630 kbar and 1300°K. According to other workers, [77] this point lies at 600 kbar and 2900°K and the boundary between graphite and diamond intersects the fusion curve at 150 kbar and 3300°K. Later, the same workers, having considered in detail the properties of elements in group IV-B and those of the isoelectronic compounds formed of elements of groups III and V, suggested that the P-T diagram of carbon should be somewhat different. [79] Figure 18a shows, as chain lines, the hypothetical boundaries between the phases proposed by these workers. In this case, the volume discontinuities in graphite, found by means of shock waves, [78] will correspond to the polymorphic transition of diamond into graphite-II.

It has also been suggested that the fusion curve of diamond should have a much smaller negative slope and that it should end at the triple point with the coordinates 600 kbar and 2700°K; the graphite-II modification should have the structure of white tin—the tetragonal body-centered type A5 lattice—and a fusion curve with a positive slope. [77] If these hypotheses are confirmed in the future, they will furnish proof of the validity of the conclusions drawn on the basis of analogies between the P-T phase diagrams of elements in the periodic system.

Figure 18b shows the P-T diagrams of silicon and germanium, found by the differential thermal analysis method. [79] The semiconductors silicon and germanium go over to the metallic state at pressures of 200 and 120 kbar, respectively. [81] Experiments showed that the slope of the fusion curve of the high-pressure phase of germanium was positive and the same sign of the slope was proposed for the fusion curve of the high-pressure phase of silicon. The structure of the high-pressure phases of these elements was investigated by x-ray diffraction and the analysis showed that they both have the white tin (type A5) lattice, which is tetragonal body-centered. [82]

As mentioned earlier, metallic or white tin has the tetragonal body-centered type A5 structure with the ratio of the axes  $c/a = 0.545$ . On cooling to 13.5°C, this lattice changes to the  $\alpha$ -Sn modification—gray

tin—which has the diamond type cubic lattice and all the properties of a semiconductor. Figure 18c shows the P-T phase diagram of tin (in accordance with [79]). The stability zone of gray tin lies at negative pressures. The phase boundaries between  $\alpha$ - and  $\beta$ -Sn and the fusion curve of  $\alpha$ -Sn have been calculated. Under pressure,  $\beta$ -Sn transforms into the Sn II modification, [83] which, as shown by x-ray diffraction investigations, has the tetragonal body-centered structure, [25] similar to the bcc type A2 structure. The possibility of a transition from the body-centered tetragonal type A5 structure to the bcc structure in tin has been considered theoretically using the concept of spatial packing [84] and has, in fact, been confirmed.

At atmospheric pressure, lead retains the fcc type A1 structure down to very low temperatures. A polymorphic transition was found in lead at 161 kbar. [85] and a study of a series of Pb-Bi alloys gave grounds for assuming that the high-pressure phase of lead had the hcp type A3 structure. [86]

Thus, considering the P-T phase diagrams of elements of the carbon group, we can note a number of characteristic features. First, we see the purely outward similarity in the diagrams. The strongly extended diagram of carbon is followed by the more compressed diagrams of silicon and germanium and the very compact diagram of tin; the “compression” occurs both along the pressure axis and along the temperature axis. The stability zone of the graphite type modification lies at negative pressures for silicon and germanium; the same is true of the diamond-type phase ( $\alpha$ -Sn) of tin. We notice also that the phases having the same structures have the same sign of the slope of the fusion curve, and only the angle of the slope changes from element to element. It would seem that the diagram of each element can be obtained by “expanding” the diagram of the neighbor which follows it in the periodic table.

Thus, having considered the phase diagram of elements in the carbon group, we may say that when the pressure is increased, the polymorphic modifications follow one another in the following sequence: hexagonal layered A9 (graphite)  $\rightarrow$  diamond A4 (diamond, Si I, Ge I,  $\alpha$ -Sn)  $\rightarrow$  tetragonal body-centered A5 (graphite-II, Si II, Ge II,  $\beta$ -Sn)  $\rightarrow$  pseudo-bcc (Sn II)  $\rightarrow$  fcc A1 (Pb)  $\rightarrow$  hcp A3 (Pb II).

The sequence of changes of the crystal structure under the influence of pressure is accompanied by an increase in the c.n. or, we may say, that when structures change under the influence of pressure the packing factor  $\varphi$  increases (this factor is equal to the ratio of the volume occupied by atoms to the total volume of a unit cell). This can be seen clearly in the adjoining table.

The observed sequence of phase diagrams suggests that the same order will apply to the sequence of changes in the high-pressure modifications in all elements of the carbon group, i.e., we may expect tin,

Sequence of changes in the crystal structure of elements of group IV-B as the pressure rises, accompanied by an increase in the c.n. and in the packing factor  $\varphi$

Lattice type	A9	A4	A5	A2	A1	A3
C. N.	3	4	6	6.2	6-6	12
$\varphi$	0.171	0.340	0.535	0.680	0.740	0.740

silicon, germanium and carbon to have a phase with an fcc or hcp type A3 structure.

9. ELEMENTS OF GROUP V-B

The phase diagrams of elements in this group also exhibit a clear sequence with increasing atomic number; this can be seen even in the very incomplete diagrams available at present.

Under normal conditions, phosphorus has several allotropic forms—white, yellow, and red phosphorus, but the greatest interest lies in the semiconducting modification, black phosphorus, which exhibits properties close to those of elements in group V-B. The orthorhombic crystal structure, with one centered face (8 atoms in a cell, c.n. = 3) of black phosphorus,

is characteristic also of one of the allotropic modifications of arsenic.

The stable form of arsenic is so-called metallic arsenic, with the rhombohedral type A7 structure. The remaining members of group V-B—antimony and bismuth—also crystallize in this structure.

Figure 19a shows a part of the P-T diagram of black phosphorus. Its fusion curve has been determined up to 20 kbar,<sup>[87]</sup> and the boundaries between the modifications are indicated only by points obtained at room temperature. The transition to P II was found from a volume discontinuity at 50 kbar<sup>[20]</sup>, using x-ray structure analysis at 80 kbar;<sup>[88]</sup> this transition was slow and was accompanied by a strong hysteresis. X-ray-diffraction studies showed that at this transition the orthorhombic layered structure of black phosphorus P I changed to the arsenic type A7 structure. Under further compression, there was another transition at 124 kbar and the resultant P III modification has the primitive cubic structure.<sup>[88]</sup>

The P-T phase diagram of arsenic is shown in Fig. 19b. Again, only certain parts of the diagram are known with certainty. The fusion curve plotted up to 60 kbar was obtained by differential thermal analysis,<sup>[89]</sup> and the polymorphic transition to the As II phase was found at 100 kbar; Bridgman's investigations of arsenic showed no volume discontinuities although he found that the volume decrement behaved

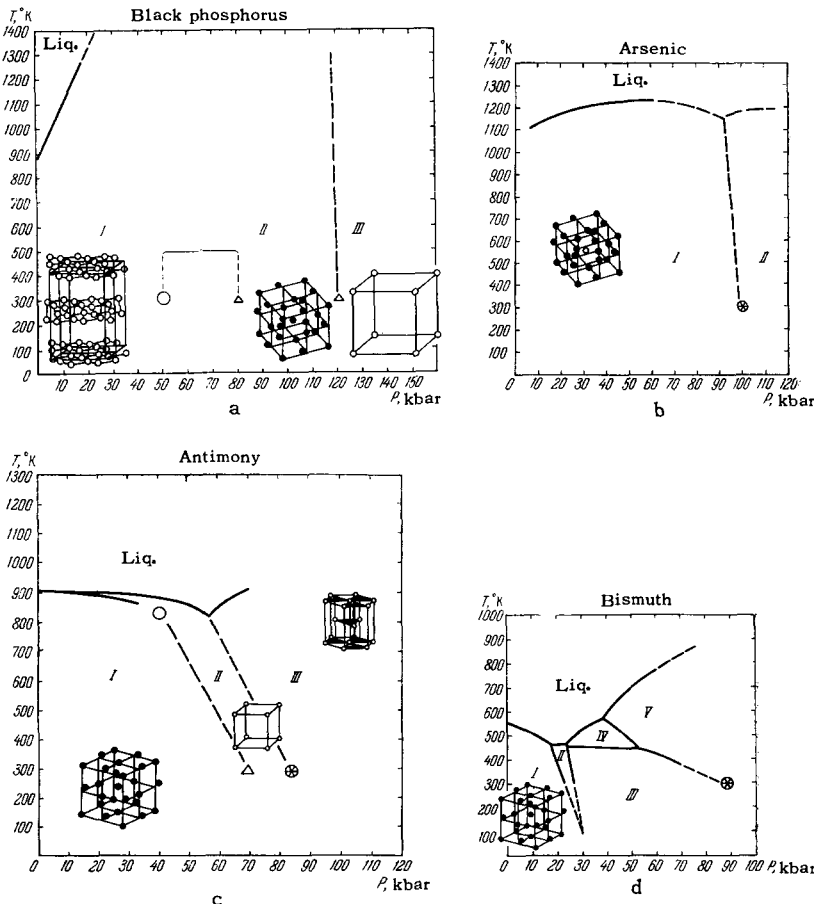


FIG. 19. a) P-T diagram of black phosphorus. The fusion curve was found by the DTA method;<sup>[87]</sup> the circle denotes conditions under which volume discontinuity was obtained,<sup>[20]</sup> and the triangles represent the coordinates of the transitions found by the x-ray diffraction method.<sup>[88]</sup> b) P-T diagram of As. The fusion curve was determined by the DTA method;<sup>[89]</sup> the "star" denotes the coordinates of polymorphic transition found from an electrical resistance discontinuity.<sup>[21]</sup> c) P-T diagram of antimony. The upper curve was reported in<sup>[89]</sup> and the lower in<sup>[87]</sup>. The circle denotes a hypothetical triple point,<sup>[87]</sup> the triangle gives the coordinates of a polymorphic transition found by x-ray structure analysis<sup>[90]</sup> and the "star" is used for the coordinates of a transition found from an electrical resistance discontinuity.<sup>[19]</sup> d) P-T diagram of bismuth, according to the DTA method.<sup>[89]</sup>

anomalously at the highest pressures produced by his apparatus, i.e., 100 kbar.<sup>[20]</sup> Bridgman found that the electrical resistance curve dropped rapidly at 100 kbar, from which he concluded that a polymorphic transition takes place at this pressure.<sup>[21]</sup> The possible boundary between normal arsenic and its high-pressure phase is shown dashed in Fig. 19b. The present author is of the opinion that the structure of the As II phase is most likely to be cubic primitive; the answer may be found by considering the P-T phase diagrams of antimony and bismuth.

Metallic antimony has the A7 type structure and is an analog of its neighbors in the group—arsenic and bismuth. At present, three modifications of antimony are known. Its fusion curve has been determined up to 70 kbar; it has a negative slope for the first two phases and a positive one for the third (Fig. 19c). One minimum has been found in the fusion curve<sup>[89]</sup> where it meets the boundary between the two solid phases, Sb II and Sb III. The lower fusion curve shown in Fig. 19c was reported in<sup>[87]</sup>. It is interesting to note that the author of the latter paper suggested that the P-T diagram of antimony should also have a triple point at the coordinates 37 kbar and 840°K. It is very likely that this hypothetical triple point does indeed exist and is a point at which the boundary between the solid phases Sb I and Sb II meets the fusion curve. The polymorphic transition Sb I-Sb II is accompanied by a very small change in volume and, therefore, it is not detected in "free plunger" apparatus which is used to determine volume discontinuities in polymorphic transitions. However, the existence of this transition was proved by an x-ray diffraction investigation.<sup>[90]</sup> When the pressure is increased to 70 kbar, the diffraction pattern of the normal modification Sb I disappears and reflections of the high-pressure phase Sb II appear. Analysis of the results shows that this modification has the primitive cubic structure. X-ray analysis also made it possible to establish the structure of the third phase of antimony—Sb III, which appeared at 85 kbar; it was found to have the hcp type A3 structure with the axis ratio  $c/a = 1.58$ .

The P-T phase diagram of bismuth has been investigated in greater detail than the diagrams of its neighbors. The diagram plotted in Fig. 19d follows<sup>[89]</sup>. This diagram indicates five polymorphic modifications coexisting in the range of pressures up to 100 kbar. It should be mentioned that Bridgman found eight modifications in this range of pressures.<sup>[37]</sup> The crystal structure is known only for normal bismuth Bi I—it is rhombohedral type A7. Several attempts have been made recently to obtain x-ray diffraction patterns of the high-pressure phases of bismuth but not all of them have been successful.<sup>[16,92-94]</sup> This is because the stability zone of the Bi II modification is very narrow. The Debye diffraction patterns obtained were probably the result of the superposition of the patterns of three bismuth modifications, Bi I, Bi II, Bi III, because

there is usually a pressure gradient in an x-ray high-pressure chamber. Moreover, it is difficult to obtain x-ray diffraction patterns of bismuth under pressure because of its exceptionally low scattering power, so that weak intensity reflections may be lost completely in the patterns obtained.

Since there are no x-ray-diffraction data on the high-pressure phases of bismuth, all we can do is to offer some suggestions about their structures. For example, it is concluded in<sup>[89]</sup> that the structure of the Bi II modification is close to the hexagonal type with three atoms in a cell because Bi-Tl alloys have a phase of the substitutional solid solution type, which has the hexagonal disordered structure. Other workers<sup>[94]</sup> are of the opinion that the lattice of the Bi II phase is very close to the bcc type because eightfold coordination has been found in liquid bismuth near the fusion curve, i.e., each atom has eight nearest neighbors<sup>[95]</sup>, and we can cite other examples when the structure of a high-pressure phase has the same coordination as the liquid near the fusion curve.

Hypotheses have also been advanced about the crystal structures of other modifications of bismuth:<sup>[94]</sup> Bi II  $\rightarrow$  A2, Bi III  $\rightarrow$  A3, Bi IV  $\rightarrow$  A2, Bi V  $\rightarrow$  A1.

We shall now consider again the P-T phase diagrams of all the elements of group V-B. They have many common features. First, there is the purely outward similarity of the diagrams which is repeated, with slight changes, from neighbor to neighbor. The slope of the fusion curves of the initial phases changes gradually from positive in the case of phosphorus to negative in the case of bismuth; it is likely that the slopes of the boundaries between the solid phases also change gradually from element to element. As the atomic number increases, the P-T diagrams tend to become compressed in the direction of lower pressures and temperatures, so that the diagram of each of these elements can be obtained by expanding or compressing the P-T diagram of its neighbor.

The most remarkable is the feature that the sequence in the crystal structure changes of the polymorphic modifications which is the same for the whole group: orthorhombic lattice with one centered face (black phosphorus PI)  $\rightarrow$  orthorhombic type A7 (P II, As, Sb, Bi)  $\rightarrow$  primitive cubic (P III, As II?, Sb II, Bi II?)  $\rightarrow$  hcp type A3 (Sb III,  $\rightarrow$  Bi III?)  $\rightarrow$  fcc type A1 (Bi V?). This sequence of structures corresponds to an increase in the coordination number of the atomic packing, i.e., an increase in the pressure provides each atom with a tighter environment of neighbors (c.n.: 3  $\rightarrow$  6  $\rightarrow$  12).

We have placed question marks against some of the modifications in the above sequence—their structures are not yet established and they may not follow the sequence. A discussion of elements of group V-B given in<sup>[96]</sup> showed that under normal conditions the energetically favored transition was from the cubic primitive to the rhombohedral type A7 structure and that

bismuth could be relatively easily, i.e., at relatively low pressures, transformed into the metallic state with the primitive cubic structure. The A7 structure can be easily pictured by representing two face-centered lattices slightly elongated along the diagonal and displaced by a very small amount with respect to each other; this amount is known as the position parameter  $u$ . In the fcc lattice, we can distinguish a unit rhombohedron having a vertex angle of  $60^\circ$ . If the two face-centered lattices are displaced until the position parameter becomes  $u = 0.250$ , we obtain a lattice with a unit cell in the form of a primitive cube. Thus, the arsenic A7 type structure represents only a small deviation from the primitive cube; this deviation is less for bismuth and greater for arsenic. High pressures destroy the A7 structure distortion and the lattice becomes primitive cubic.

Thus, if bismuth is placed in a general sequence of elements in group V-B, we may expect the following sequence of structural changes: Bi I—rhombohedral type A7; Bi II—primitive cubic; Bi III—hcp type A3; Bi IV—bcc; Bi V—fcc.

## 10. ELEMENTS OF GROUP VI-B

Of the VI-B elements, we shall consider only selenium and tellurium because of the great similarity of their properties and because more data are available on their P-T phase diagrams than for the other elements. Under normal conditions, selenium has several allotropic modifications, but the thermodynamically stable form is gray selenium, having the hexagonal type A8 structure; tellurium crystallizes in the same structure.

In the type A8 packing, each atom has two nearest neighbors, one above and one below, both lying on a common vertical, so that the whole structure splits into vertical helical chains.

It is interesting to note that the type A8 (selenium) and type A7 (arsenic) structures are both based on a three-layered cubic packing, but the distortion of the cube is in opposite directions for these two types of structure. In a normal cube, the primitive rhombohedron has the vertex angle of  $60^\circ$ , in the type A7 structure (arsenic, antimony, and bismuth) this angle

is less than  $60^\circ$ , while in the type A8 structure it is greater than  $60^\circ$ .

It is evident from Fig. 20a that the P-T diagram of selenium has not been investigated much. The fusion curve has been determined only to 10 kbar,<sup>[97]</sup> and the polymorphism under pressure is indicated by a kink in the dependence of the volume decrement on pressure at 63 kbar<sup>[37]</sup> and by electrical resistance discontinuities at 46 kbar<sup>[21]</sup> and 128 kbar.<sup>[98]</sup> The first two discontinuities probably represent the same transition Se I  $\rightarrow$  Se II, and the boundary between these phases should be drawn as shown dashed in our figure. The fusion curve of the Se II phase and the phase boundary between Se II and Se III are equally hypothetical.

The P-T phase diagram of tellurium has been determined more fully; it is shown in Fig. 20b. Its fusion curve<sup>[99]</sup> has been determined up to 50 kbar and it has one deep minimum at 30 kbar, which is the point of intersection of the fusion curve with the equilibrium boundary between the phases Te II and Te III; a maximum in the fusion curve of Te was reported in<sup>[100]</sup>. The Te I  $\rightarrow$  Te II transition is accompanied by a very small volume change, which is so small that having plotted the phase boundary between the modifications Te I and Te II, Bridgman suggested that his results were not to be taken too seriously.<sup>[68]</sup> On further increase of pressure, two more transitions take place in tellurium at 45 and 70 kbar; these transitions are accompanied by very marked changes in the volume<sup>[137]</sup> and the electrical resistance.<sup>[101]</sup> It is interesting to note that x-ray diffraction analysis showed a polymorphic transition at 15 kbar.<sup>[102]</sup> It was found that the chain-like type A8 structure of normal tellurium transformed under pressure into the layered structure of the A7 arsenic type; this transition was not accompanied by a volume discontinuity or a change in density.

It is possible that the phase boundary Te I-Te II emerges at the maximum of the fusion curve. Further changes in the structure occur at 45 kbar; this is clear from the Debye diffraction pattern which was obtained for the Te III phase under pressure; it has not yet been possible to interpret this pattern.<sup>[102]</sup> If we now compare the P-T phase diagrams of selenium and tellurium, we see that they follow the general

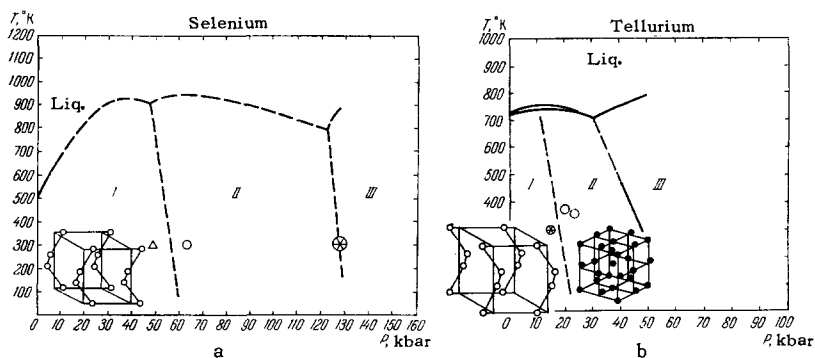


FIG. 20. a) Probable P-T diagram of Se. The fusion curve was determined from volume discontinuities;<sup>[97]</sup> the coordinates of the polymorphic transitions are indicated as follows: the circle shows a kink in the pressure dependence of the volume decrement,<sup>[37]</sup> The "star" and the triangle denote electrical resistance discontinuities.<sup>[21,98]</sup> b) P-T phase diagram of tellurium plotted by the DTA method.<sup>[99,100]</sup> The "star" denotes the coordinates of the polymorphic transition Te I-Te II, found by the x-ray diffraction method.<sup>[102]</sup> The circles and part of the phase boundary between Te II and Te III were obtained by investigating the volume decrement under pressure.<sup>[68]</sup>

rule: the tellurium diagram is a compressed variant of the selenium diagram. This suggests that selenium should have the same polymorphism as tellurium, i.e., A8  $\rightarrow$  A7.

It should be mentioned also that these two elements should have a modification with the primitive cubic structure, since polonium, which follows tellurium in the same group, has this structure.

## 11. IRON GROUP

The P-T phase diagram of iron has been investigated over a very wide range of pressures and temperatures. At atmospheric pressure the stable modification of  $\alpha$ -Fe has the bcc structure up to 1179°K, which is then replaced by the  $\gamma$ -Fe phase with the fcc structure. Further heating (to T = 1674°K) changes the fcc phase into the high-temperature form  $\delta$ -Fe, which, like the majority of high-temperature modifications, has the type A2 structure, which is bcc.

Figure 21 shows the P-T phase diagram of iron, which represents the results of analyses of very many investigations.<sup>[103]</sup> The equilibrium curve between the  $\alpha$ - and  $\gamma$ -phases has been investigated by a large number of workers. It has been determined dilatometrically,<sup>[104]</sup> from electrical resistance anomalies,<sup>[105,106]</sup> heats of  $\alpha \rightarrow \gamma$  transition,<sup>[107]</sup> thermal conductivity discontinuity,<sup>[106]</sup> and using shock waves.<sup>[108,109]</sup>

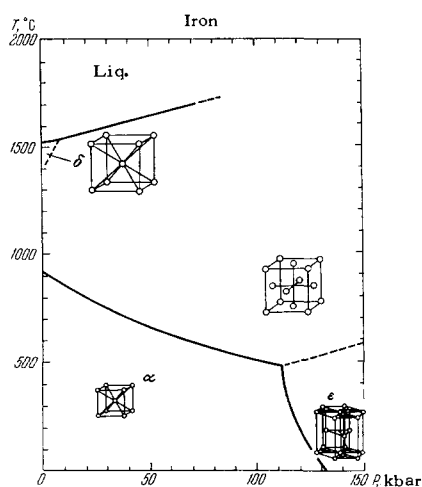


FIG. 21. The P-T phase diagram of iron. The fusion curve was determined by the DTA method.<sup>[110]</sup> The  $\alpha$ - $\gamma$  and  $\alpha$ - $\epsilon$  boundaries were plotted using various methods, and the  $\gamma$ - $\delta$  and  $\gamma$ - $\epsilon$  phase boundaries were calculated in<sup>[103]</sup>.

The sudden change in the slope of this boundary has suggested that the phase diagram has a triple point and that, in addition to the  $\alpha$ - and  $\gamma$ -phases, there is one further modification of iron; it is called  $\epsilon$ -Fe by analogy with the  $\epsilon$ -phase for cobalt.

The existence of this phase was proved by x-ray-structure analysis which showed that  $\epsilon$ -Fe had the hcp type A3 structure.<sup>[103,17]</sup>

The  $\gamma$ - $\delta$  and  $\gamma$ - $\epsilon$  phase boundaries have not been determined experimentally but they have been calculated;<sup>[103]</sup> the fusion curve was determined by the differential thermal analysis.<sup>[110]</sup> The  $\epsilon$ -phase of iron is probably stable to very high pressures; the application of shock waves up to 4000 kbar showed no sudden changes in density.<sup>[111]</sup>

We shall now turn to the neighbors of iron: cobalt and nickel. Under normal conditions, cobalt has two modifications: the hexagonal type A3 ( $\epsilon$ -Co), stable up to 755°K, which is replaced by a high-temperature  $\gamma$ -phase with the fcc structure (type A1) stable right up to the melting point. No polymorphism has been found in nickel; it has the fcc type A1 structure.

As in all cases considered earlier, we can say that the P-T phase diagrams of the iron group are shifted toward lower pressures and temperatures on increase of the atomic number. The fcc and hexagonal phases, coexisting in iron under high pressures, exhibit a transition at atmospheric pressure in cobalt; the temperature of this transition is lower than in iron.

The practical conclusion of such an analysis is that at some pressure we would expect nickel to have an  $\epsilon$ -phase with the hcp type A3 structure.

The P-T phase diagrams have not yet been constructed for all the elements of the periodic table and, therefore, in generalizing the known facts, we are forced to ignore many interesting substances.

Knowledge of the P-T diagrams allows us to obtain information on transitions which alter the crystal structure; moreover, using the available sequences of polymorphic modifications within each group of the periodic table, we can even now make some predictions of structures which have not yet been investigated by x-ray-diffraction or structures of high-pressure modifications which are difficult to produce. Furthermore, the knowledge of crystal structures of high-pressure phases or at least predictions of such structures will help in the search for new substances under pressure if the properties are known in advance.

\* \* \*

Having considered the P-T phase diagrams of some elements in the periodic table, we have been able to establish that their periodicity applies also to the phase diagrams. We have been able to show that the P-T diagrams of elements in one group are very similar, but they gradually "contract" moving toward lower pressures and temperatures as the atomic number increases. The variety of elements is reflected in the variety of forms of the phase boundaries. The general tendency in the polymorphism of elements produced by the application of pressure is the sequence in which looser crystal structures are followed by more closely packed structures, having higher coordination numbers. Against the background of this general rule, we can point out a number of cases in which the application of pressure alters a structure



with a higher packing factor to a structure with a lower value of this factor  $\varphi$ . In some cases, electronic transitions are not accompanied by a change in the crystal structure, as, for example, in the case of cerium at 7 kbar, cesium at 42.5 kbar, and possibly barium at 17 kbar. It is worth noting that the sequence of changes in the crystal structure is the same for all elements in a group and, moreover, that in many groups this sequence is the same as that sequence of structures obtained in a group for increasing atomic numbers.

In some cases, it is found that the P-T diagram of an element has much in common with the diagrams of elements in the neighboring group, for example, the diagram of barium is similar to the diagrams of alkali metals.

It should also be mentioned that predictions of the form of the crystal structure of a high-pressure modification may be based on such information as the existence of similar structures in solid solutions of these elements, the value of the volume change at a transition, and the form of the electrical resistance curve in the region of the transition; another important point is that, in many cases, the coordination number of a high-pressure phase is equal to the coordination number of the liquid phase near the fusion curve.

All this, taken together, has been used to predict possible structures of high-pressure modifications of some elements. It is probable that beryllium has the bcc structure after a transition at 93 kbar and that calcium also changes to the bcc structure at 375 kbar. Mercury may have a hcp magnesium type phase, and gallium and indium are likely to have a transition to the fcc structure without a change in volume. All the elements of group IV-A may have phases with the hcp structure, and this applies to carbon as well. In the case of elements in groups V-A and VI-A, we may expect modifications with the cubic primitive structure and nickel should have a high-pressure phase with the hcp structure.

Similar relationships may be observed not only in the P-T phase diagrams of elements but also in the diagrams of some simple compounds—in particular, alkali-metal halides, AB-type compounds, oxides and similar substances.

<sup>1</sup>L. F. Vereshchagin and A. I. Likhter, DAN SSSR **86**, 745 (1952).

<sup>2</sup>Yu. N. Ryabinin, DAN SSSR **104**, 721 (1955).

<sup>3</sup>P. Gombas, *Statistical Theory of the Atom and Its Applications* (Russ. Transl., Moscow, IL, 1951). [Springer-Wien, 1947]

<sup>4</sup>A. Lawson and Ting Yuan Tang, *Phys. Rev.* **76**(2), 325 (1949).

<sup>5</sup>R. Sternheimer, *Phys. Rev.* **78**, 235 (1950).

<sup>6</sup>A. F. Kapustinskii, *Izv. AN SSSR, OKhN*, No. 5, 427 (1956).

<sup>7</sup>A. A. Abrikosov, *JETP* **39**(6), 1797 (1960), *Soviet Phys. JETP* **12**, 1254 (1961).

<sup>8</sup>J. H. Poynting, *Phil. Mag.* **12**, 32, 232 (1881).

<sup>9</sup>A. Eucken and F. M. Müller-Poilleys, *Lehrbuch der Physik*, Braunschweig, Vieweg, 1926, Vol. 3(1), p. 492.

<sup>10</sup>G. Tamman, *Ann. Physik* **37**, 975 (1912).

<sup>11</sup>P. W. Bridgman, *Phys. Rev.* **6**, 1 (1915).

<sup>12</sup>C. Domb, *Nuovo Cimento* **9**, Suppl. 9 (1958).

<sup>13</sup>F. E. Simon, *Farnas Memorial Volume, Research Council of Israel*, No. 1, Special Publ., Jerusalem, 1952, p. 37.

<sup>14</sup>J. C. Jamieson and A. W. Lawson, in collection: *Modern Very High Pressure Technique*, ed. by R. H. Wentorff, Jr., Butterworths, London, 1962 (Russ. Transl., "Mir," M., 1964), p. 118.

<sup>15</sup>L. F. Vereshchagin, in C. A. Swenson's *Physics of High Pressures* (Russ. Transl., IL, M., 1963), p. 325.

<sup>16</sup>G. J. Piermarini and C. W. Weir, *J. Res. Nat. Bur. Stand.* **A66**, 325 (1962).

<sup>17</sup>J. C. Jamieson and A. W. Lawson, *J. Appl. Phys.* **33**(3), 776 (1962).

<sup>18</sup>E. A. Perez-Albuerne, K. F. Forsgren, and H. G. Drickamer, *Rev. Sci. Instrum.* **35**(1), 29 (1964).

<sup>19</sup>J. D. Barnett and H. T. Hall, *Rev. Sci. Instrum.* **35**(2), 175 (1964).

<sup>20</sup>P. W. Bridgman, *Proc. Am. Acad. Arts Sci.* **76**(3), 71 (1948).

<sup>21</sup>P. W. Bridgman, *Proc. Am. Acad. Arts Sci.* **81**, 165 (1952).

<sup>22</sup>H. T. Hall, L. Merrill, and J. D. Barnett, *Science* **146** (No. 3649), 1297 (1964).

<sup>23</sup>G. C. Kennedy, A. Jayaraman, and R. C. Newton, *Phys. Rev.* **126**(4), 1363 (1962).

<sup>24</sup>R. A. Stager and H. G. Drickamer, *Phys. Rev. Letters* **12**(1), 19 (1964).

<sup>25</sup>J. D. Barnett, R. B. Bennion, and H. T. Hall, *Science* **141** (No. 3585), 1041 (1963).

<sup>26</sup>J. C. Jamieson, *Bull. Geol. Soc. Amer.*, Horston Meeting, November, 1962.

<sup>27</sup>G. C. Kennedy, A. Jayaraman, and R. C. Newton, *J. Geophys. Res.* **67**(6), 2559 (1962).

<sup>28</sup>R. A. Stager and H. G. Drickamer, *Phys. Rev.* **132**(1), 124 (1963).

<sup>29</sup>C. S. Barrett, *Acta Cryst.* **9**, 671 (1956).

<sup>30</sup>F. P. Bundy, *Phys. Rev.* **115**, 274 (1959).

<sup>31</sup>G. C. Kennedy and P. N. LaMori, in collection: *Progress in Very High Pressure Research* (ed. by F. P. Bundy), John Wiley and Sons, New York, 1962, p. 304.

<sup>32</sup>E. S. Alekseev and R. G. Arkhipov, *FTT* **4**(5), 1077 (1962).

<sup>33</sup>A. J. Martin and A. Moore, *J. Less-common Metals* **1**, 85 (1959).

<sup>34</sup>A. R. Marder, *Science* **142** (No. 3593), 664 (1963).

<sup>35</sup>R. A. Stager and H. G. Drickamer, *Phys. Rev.* **131**(6), 2524 (1963).

<sup>36</sup>A. Jayaraman, W. Klement, Jr., and G. C. Kennedy, *Phys. Rev.* **132**(4), 1620 (1963).

- <sup>37</sup> P. W. Bridgman, Proc. Am. Acad. Arts **74**, 425 (1942).
- <sup>38</sup> J. F. Smith, O. N. Carlson, and R. W. West, J. Electrochem. Soc. **103**, 409 (1956).
- <sup>39</sup> D. B. McWhan and A. Jayaraman, Appl. Phys. Letters **3**(8), 129 (1963).
- <sup>40</sup> A. Jayaraman, W. Klement, Jr., and G. C. Kennedy, Phys. Rev. Letters **10**(9), 387 (1963).
- <sup>41</sup> B. C. Deaton and D. E. Bowen, Appl. Phys. Letters **4**(6), 97 (1964).
- <sup>42</sup> P. W. Bridgman, Proc. Am. Acad. Arts Sci. **72**(5), 207 (1938).
- <sup>43</sup> J. D. Barnett, R. B. Bennion, and H. T. Hall, Science (No. 3580) 534 (1963).
- <sup>44</sup> P. W. Bridgman, Proc. Am. Acad. Arts Sci. **60**, 346 (1925).
- <sup>45</sup> V. P. Butuzov, E. G. Ponyatovskii, and G. I. Shakhovskii, DAN SSSR **109**(3), 519 (1956).
- <sup>46</sup> J. C. Jamieson, J. Geol. **65**(3), 334 (1957).
- <sup>47</sup> N. Thompson and D. J. Millard, Phil. Mag. **43**, 422 (1952).
- <sup>48</sup> W. Klement, Jr., A. Jayaraman, and G. C. Kennedy, Phys. Rev. **131**(1), 1 (1963).
- <sup>49</sup> M. Atoji, J. E. Schirber, and C. A. Swenson, J. Chem. Phys. **31**(6), 1628 (1959).
- <sup>50</sup> E. G. Ponyatovskii, DAN SSSR **120**(5), 1021 (1958), Soviet Phys. Doklady **3**, 498 (1959).
- <sup>51</sup> L. D. Livshitz, Yu. S. Genshaft, and V. K. Markov, JETP **43**(4), 1262 (1962), Soviet Phys. JETP **16**, 894 (1963).
- <sup>52</sup> B. L. Davis and L. H. Adams, Solid State Comm. **1**(7), 241 (1963).
- <sup>53</sup> A. Jayaraman, Phys. Rev. **A137**(1), 179 (1965).
- <sup>54</sup> D. McWhan, P. W. Montgomery, H. D. Stromberg, and G. Jura, J. Phys. Chem. **67**(11), 2308 (1963).
- <sup>55</sup> G. J. Piermarini and C. E. Weir, Science **144** (No. 3614), 69 (1964).
- <sup>56</sup> P. W. Bridgman, Proc. Am. Acad. Arts Sci. **71**, 387 (1936).
- <sup>57</sup> A. Jayaraman and R. C. Sherwood, Phys. Rev. Letters **12**(1), 22 (1964).
- <sup>58</sup> A. Jayaraman and R. C. Sherwood, Phys. Rev. Letters **12**(10), 3 (1964).
- <sup>59</sup> R. B. Aust and H. G. Drickamer, Science **140** (No. 3568), 817 (1963).
- <sup>60</sup> R. H. Wentorff and J. S. Kasper, Science **139** (No. 3552), 338 (1963).
- <sup>61</sup> P. W. Bridgman, Proc. Am. Acad. Arts Sci. **82**, 95 (1953).
- <sup>62</sup> R. A. Stager and H. G. Drickamer, Phys. Rev. **133**, 830 (1964).
- <sup>63</sup> A. Jayaraman, Phys. Rev. **A135**(4), 1056 (1964).
- <sup>64</sup> H. T. Hall, J. D. Barnett, and L. Merrill, Science **139**, 111 (1963).
- <sup>65</sup> A. Jayaraman, W. Klement, Jr., and G. C. Kennedy, J. Phys. Chem. Solids **24**, 7 (1963).
- <sup>66</sup> L. F. Vereshchagin, S. S. Kabalkina, and Z. D. Troitskaya, DAN SSSR **158**(5), 1265 (1964).
- <sup>67</sup> W. B. Pearson, in collection: Handbook of Lattice Spacings and Structures of Metals and Alloys, Pergamon Press, New York, 1958, p. 692.
- <sup>68</sup> P. W. Bridgman, Phys. Rev. **48**, 893 (1935).
- <sup>69</sup> L. Kaufman, Acta Met. **9**, 896 (1961).
- <sup>70</sup> E. Parthe, Z. Krist. **115**, 52 (1961).
- <sup>71</sup> A. Jayaraman, W. Klement, Jr., and G. C. Kennedy, Phys. Rev. **131**(2), 644 (1963).
- <sup>72</sup> L. Kaufman, Acta Met. **7**, 575 (1959).
- <sup>73</sup> J. C. Jamieson, Science **140** (No. 3562), 72 (1963).
- <sup>74</sup> Yu. A. Bogaryatskii, G. I. Rozova, and V. V. Saganova, DAN SSSR **105**(6), 1225 (1955).
- <sup>75</sup> B. A. Hatt and J. A. Roberts, Acta Met. **8**, 575 (1960).
- <sup>76</sup> F. P. Bundy, Science **137**, 1057 (1962).
- <sup>77</sup> A. Jayaraman, R. C. Newton, and G. C. Kennedy, International Conference on Diamonds, Paris, 1962.
- <sup>78</sup> B. J. Alder and R. H. Christian, Phys. Rev. Letters **7**, 367 (1961).
- <sup>79</sup> A. Jayaraman, W. Klement, Jr., and G. C. Kennedy, Phys. Rev. **130**(2), 540 (1963).
- <sup>80</sup> G. A. Samara and H. G. Drickamer, J. Chem. Phys. **37**, 471 (1962).
- <sup>81</sup> S. Minomura and H. G. Drickamer, J. Phys. Chem. Solids **29**, 451 (1962).
- <sup>82</sup> J. C. Jamieson, Science **139** (No. 3556), 762 (1963).
- <sup>83</sup> R. A. Stager, A. S. Balchan, and H. G. Drickamer, J. Chem. Phys. **37**(5), 1154 (1962).
- <sup>84</sup> M. J. P. Musgrave, J. Phys. Chem. Solids **4**, 557 (1963).
- <sup>85</sup> A. S. Balchan and H. G. Drickamer, Rev. Sci. Instrum. **32**, 308 (1961).
- <sup>86</sup> W. Klement, Jr., J. Chem. Phys. **38**, 298 (1963).
- <sup>87</sup> V. P. Butuzov, Kristallogr. **2**, 536 (1957).
- <sup>88</sup> J. C. Jamieson, Science **139**, (No. 3561), 1291 (1963).
- <sup>89</sup> W. Klement, Jr., A. Jayaraman, and G. C. Kennedy, Phys. Rev. **131**(2), 632 (1963).
- <sup>90</sup> S. S. Kabalkina, L. F. Vereshchagin, and V. P. Mylov, DAN SSSR **152**(3), 585 (1963), Soviet Phys. Doklady **8**, 917 (1964).
- <sup>91</sup> L. F. Vereshchagin, A. A. Semerchan, N. N. Kuzin, and S. V. Popova, DAN SSSR **136**, 32 (1961).
- <sup>92</sup> L. F. Vereshchagin and I. V. Brandt, DAN SSSR **108**(3), 423 (1956), Soviet Phys. Doklady **1**, 312 (1957).
- <sup>93</sup> J. C. Jamieson, A. W. Lawson, and N. D. Nachtrieb, Rev. Scient. Instrum. **30**(11), 1016 (1959).
- <sup>94</sup> J. C. Jamieson and A. W. Lawson, in: Modern Very High Pressure Technique (ed. by R. H. Wentorff, Jr.), Butterworths Scient. Publ. London, 1962, p. 70.
- <sup>95</sup> P. C. Sharrach, J. I. Petz, and R. F. Kruch, J. Chem. Phys. **32**, 241 (1960).
- <sup>96</sup> A. A. Abrikosov and L. A. Fal'kovskii, JETP **43**, 1089 (1962), Soviet Phys. JETP **16**, 769 (1963).
- <sup>97</sup> S. E. Babb, Jr., J. Chem. Phys. **37**(4), 922 (1962).
- <sup>98</sup> A. S. Balchan and H. G. Drickamer, J. Chem. Phys. **34**(6), 1948 (1961).
- <sup>99</sup> G. C. Kennedy and R. C. Newton, in: Solids under Pressure (ed. by W. Paul and D. M. Warschauer),

McGraw-Hill, New York, 1963, p. 171.

<sup>100</sup> N. A. Tikhomirova and S. M. Stishov, JETP **43**, 232 (1962), Soviet Phys. JETP **16**, 1639 (1963).

<sup>101</sup> P. W. Bridgman, Proc. Am. Acad. Arts Sci. **81**, 233 (1952).

<sup>102</sup> S. S. Kabalkina, L. F. Vereshchagin, and B. M. Shulenin, JETP **45**(6), 2073 (1963), Soviet Phys. JETP **18**, 1422 (1964).

<sup>103</sup> T. Takachashi and W. A. Bassett, Science **145** (No. 3631), 483 (1964).

<sup>104</sup> F. Birch, Amer. J. Sci. **238**, 192 (1940).

<sup>105</sup> L. Kaufman, A. Leyenaar, and J. S. Harvey, in: Progress in Very High Pressures Research (ed. by F. P. Bundy), John Wiley and Sons, New York, 1962, p. 90.

<sup>106</sup> E. V. Clougherty and L. Kaufman, in: High Pressure Measurement (ed. by Giardini and Lloyd), Butterworths, Washington, 1963, p. 152.

<sup>107</sup> G. C. Kennedy and R. C. Newton, in: Solids under Pressure (ed. by W. Paul and D. M. Warschauer), McGraw-Hill, New York, 1963, p. 163.

<sup>108</sup> J. D. Barnett, E. C. Peterson, and S. Minshall, J. Appl. Phys. **27**, 291 (1956).

<sup>109</sup> P. C. Johnson, B. A. Stein, and R. S. Davis, J. Appl. Phys. **33**, 557 (1962).

<sup>110</sup> H. M. Strong, in: High Pressure Research (ed. by F. P. Bundy), John Wiley and Sons, New York, 1961, p. 182.

<sup>111</sup> L. V. Al'tshuler, K. K. Krupnikov, V. N. Ledenev, V. I. Shchuchikhin, and M. I. Brazhnik, JETP **34**, 874 (1958), Soviet Phys. JETP **7**, 606 (1958).

<sup>112</sup> I. S. Bolgov, Yu. N. Smirnov, and V. A. Finkel', FMM **17**, 877 (1964).

Translated by A. Tybulewicz